

# The Supercluster–Void Network.

## IV. The Shape and Orientation of Superclusters

Jaak Jaaniste<sup>1</sup>, Erik Tago<sup>1</sup>, Maret Einasto<sup>1</sup>, Jaan Einasto<sup>1</sup>, Heinz Andernach<sup>2</sup> and Volker Müller<sup>3</sup>

<sup>1</sup> Tartu Observatory, EE-2444 Tõravere, Estonia

<sup>2</sup> Depto. de Astronomía, IFUG, Apdo. Postal 144, 36000 Guanajuato, Mexico

<sup>3</sup> Astrophysical Institute Potsdam, An der Sternwarte 16, D-14482 Potsdam, Germany

Received ... 1997 / Accepted ... 1997

**Abstract.** We present a study of the shape, size, and spatial orientation of superclusters of galaxies. Approximating superclusters by triaxial ellipsoids we show that superclusters are flattened, triaxial objects. We find that there are no spherical superclusters. The sizes of superclusters grow with their richness: the median semi-major axis of rich and poor superclusters (having  $\geq 8$  and  $< 8$  member clusters) is 42 and 31  $h^{-1}$  Mpc, respectively. Similarly, the median semi-minor axis is 12 and 5  $h^{-1}$  Mpc for rich and poor superclusters. The spatial orientation of superclusters, as determined from the axes of ellipsoids, is nearly random. We do not detect any preferable orientation of superclusters, neither with respect to the line of sight, nor relative to some other outstanding feature in the large scale structure, nor with respect to the directions of principal axes of adjacent superclusters.

**Key words:** cosmology: observations — large-scale structure of the Universe

### 1. Introduction

Superclusters of galaxies represent the largest relatively isolated density enhancements in the Universe with a characteristic size up to  $\approx 100 h^{-1}$  Mpc (Oort 1983, Einasto *et al.* 1994, hereafter EETDA). Superclusters evolve from density perturbations near the maximum of the power spectrum (Frisch *et al.* 1995). Thus the study of superclusters, their shapes, dimensions, spatial distribution and orientations gives us information about the formation and evolution of the Universe on the largest scales.

In the present series of papers we investigate the properties and the distribution of superclusters traced by rich clusters of galaxies. In the first paper of the series (Einasto

*et al.* 1997b, Paper I) we constructed a new catalogue of superclusters up to a redshift of  $z = 0.12$ ; this catalogue contains 220 superclusters with at least two member clusters. In Paper I we also investigated the large-scale distribution of superclusters, and showed that superclusters and voids form a rather regular network with a characteristic scale of about 120  $h^{-1}$  Mpc. In the following papers we determined the correlation function of clusters of galaxies (Einasto *et al.* 1997c,d, Papers II and III), and the power spectrum of clusters of galaxies (Einasto *et al.* 1997a).

In the present paper we concentrate on the properties of superclusters themselves: their form, dimension and orientation. So far the shapes and orientations of superclusters have been studied only in a few papers. West (1989) analysed 11 superclusters with at least 5 members, Plionis *et al.* (1992) investigated the shapes of a small number of superclusters, and Zucca *et al.* (1993, hereafter ZZSV) studied line-of-sight orientations of superclusters, as well as velocity dispersions of clusters in superclusters, but not the supercluster shapes.

Superclusters can be approximated by triaxial ellipsoids, and we shall determine both the length and the orientation of major and minor semi-axes of these ellipsoids. In Papers II and III of this series we describe how the correlation length of our cluster samples depend on the richness of superclusters they belong to. In this paper we analyse the sizes of superclusters of different richness.

We also study the large-scale orientations of superclusters. We shall check for the presence of a preferred orientation of superclusters with respect to the line of sight. Such an orientation could indicate the presence of contaminations in the catalogue of clusters, or the influence of cluster peculiar velocities and cluster movements from void interiors toward void walls. We also look for other effects like e.g. possible correlations in the supercluster orientation connected with well-known features of the large-scale structure, such as the Shapley supercluster, the Bootes

Send offprint requests to: J. Jaaniste

void, or the Dominant Supercluster Plane described in Paper I.

So far several different kinds of preferred orientations of galaxies and systems of galaxies have been found – the alignment of major axes of brightest galaxies in clusters and superclusters with the major axis of galaxy systems and the alignment of major axes of clusters in superclusters to be parallel with the main ridge of superclusters (Jõeveer and Einasto 1978, Einasto *et al.* 1980, Gregory *et al.* 1981, Binggeli 1982, Djorgovski 1983, Flin and Godlowski 1986, West 1989). We check for the presence of pairwise correlation for superclusters in order to see whether such alignments extend over larger scales than detected earlier.

The paper is organised as follows. In Section 2 we describe the catalogue of superclusters used in this study. In Section 3 we describe the method to find the shapes of superclusters, in Section 4 we study the properties of the superclusters (shape and size), and in Section 5 we discuss the orientation of superclusters. The paper concludes with a summary of principal results.

We denote with  $h$  the Hubble constant in units of 100 km s<sup>-1</sup> Mpc<sup>-1</sup>.

## 2. Data

### 2.1. The supercluster catalogue

We shall use the catalogue of superclusters determined in Paper I which is based on the compilation of all available redshift determinations of rich clusters of galaxies, catalogued by Abell (1958), and Abell, Corwin and Olowin (1989). The cluster dataset has been described by Andernach, Tago and Stengler-Larrea (1995) and Andernach and Tago (1998). To construct the supercluster catalogue we used 1304 clusters of all richness classes up to a redshift of  $z = 0.12$ . Of these clusters about 2/3 have measured redshifts, while for the rest photometric distances have been estimated on the basis of the 10th brightest member of the cluster. The catalogue of superclusters in Paper I contains all systems with at least 2 member clusters, in total 220 superclusters. For details of the whole catalogue we refer to Paper I. For the present study we use only superclusters with at least 5 members, and with a minimum of three members having spectroscopically measured redshifts, in total 42 superclusters. In Table A1 we give basic data for the superclusters analysed below: the identification number and multiplicity (as given in Paper I), and data on the shape and orientation.

In Paper I we showed that rich superclusters are located in chains and walls, the most prominent of these being the Dominant Supercluster Plane. This plane is almost parallel to the supergalactic YZ plane and lies in a narrow supergalactic X interval,  $-75 < X < 25 h^{-1}$  Mpc. In Section 5 we study the orientations of superclusters with respect to this plane.

## 3. Ellipsoid of concentration

### 3.1. Method

Here we describe the method we applied to determine the shape and the size of rich superclusters, and its stability.

Superclusters are not regular systems with well-defined boundaries but aggregates of quite sparsely distributed clusters with some central concentration. Therefore we have to find a mathematical method to determine a geometrical figure or body that approximates the distribution of clusters in superclusters. One of such bodies, a rectangular brick, aligned in the direction of supergalactic coordinates, was used in EETDA to estimate the size of superclusters. However, this approach does not give us any information about the orientation of superclusters.

For our purpose the 3-dimensional ellipsoid is more suitable. There are several methods to determine such ellipsoids, two of them have been used earlier to study the symmetry of clustering. Jaaniste (1982) used the ellipsoid of concentration to study the distribution of the companions of our Galaxy; West (1989) used the inertia ellipsoid to study the morphology of superclusters.

In the present study we use the classical ellipsoid of concentration (see e.g. Korn and Korn 1961), centred on the geometrical centre of the supercluster:

$$\sum_{i,j=1}^3 (\lambda_{ij})^{-1} x_i x_j = 5, \quad (1)$$

where

$$\lambda_{ij} = \frac{1}{N_{cl}} \sum_{l=1}^{N_{cl}} (x_i^l - \xi_i)(x_j^l - \xi_j), \quad (2)$$

is the covariance matrix for the non-weighted distribution;  $\xi_i = \frac{1}{N_{cl}} \sum_{l=1}^{N_{cl}} x_i^l$  are the Cartesian coordinates of the geometrical centre of the supercluster, and  $N_{cl}$  is the multiplicity of the supercluster. The formula determines a 3-dimensional ellipsoidal surface with the distance from the centre of the ellipsoid equal to the rms deviation of supercluster members in the corresponding direction. More correctly a mathematician defines the ellipsoid of concentration so that "a uniform distribution function within it has the same covariance matrix as the given distribution". One of these ellipsoids, calculated for the Shapley supercluster, is shown as an example in Figure 1.

The ellipsoid, given by the standard formula of a quadric surface, allows us to find the principal axes of the superclusters, their spatial orientation, the spatial extent and volume for all superclusters with  $N_{cl} \geq 5$ . For smaller groups the method cannot be applied due to the small number of independent coordinates.

In Table A1 we present the main parameters of the ellipsoid of concentration of each supercluster studied: the reference number,  $No$ , from Table A1 of Paper I; the number of member clusters,  $N_{cl}$ ; the length of the three principal semi-axes:  $c$ ,  $b$  and  $a$ ; the ellipticity,  $e$ , defined as

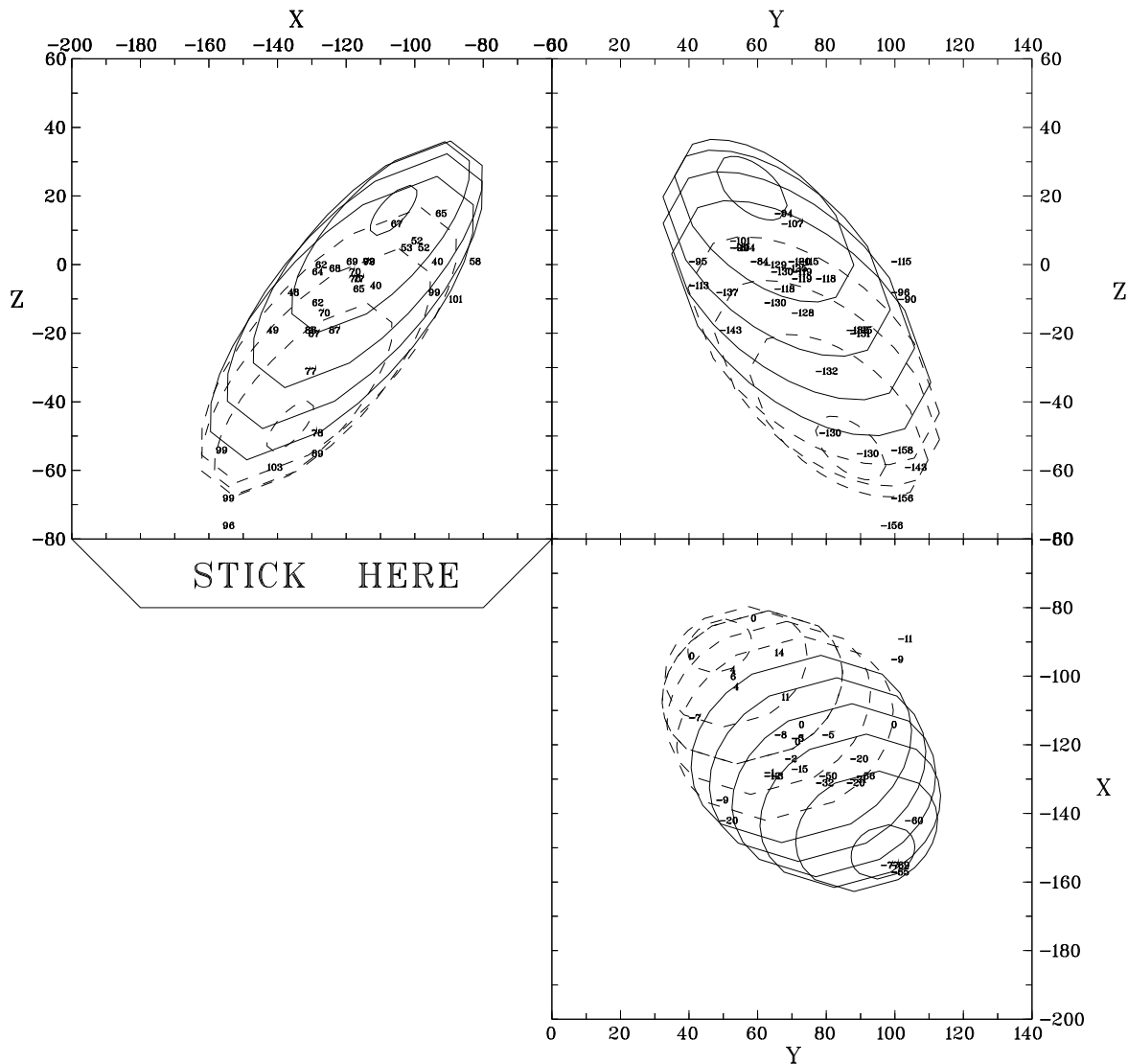


**Fig. 1.** The Shapley supercluster ellipsoid. Ellipses are the intersections of the ellipsoid with the planes parallel to corresponding coordinate plane; the dashed ones correspond to the far side of the ellipsoid. The numbers in each panel (view) indicate the third coordinate and are plotted at the position of the corresponding supercluster member. Six clusters seen in the lower parts of each panel probably do not belong to the main body of the supercluster.

the ratio of the volume of the ellipsoid to the volume of the sphere with radius equal to the major semi-axis,  $V = \frac{4\pi}{3}abc$  to  $V_{sph} = \frac{4\pi}{3}a^3$ ; the angles of the ellipsoids' minor and major axes ( $\angle cx$ , and  $\angle ax$ ) with respect to the supergalactic  $X$ -axis, and to the line of sight ( $\angle cr$ ,  $\angle ar$ ).

### 3.2. Stability of the method

It is clear that parameters of the ellipsoid depend on the number and location of clusters in the supercluster. To study this dependence we exclude members of a supercluster one by one and recalculate the parameters of the ellipsoid once again at each step. In this manner we reduce the multiplicity down to a minimum  $N_{cl}$  of four. For

smaller  $N_{cl}$  the ellipsoid cannot be determined. We studied four real and two artificial superclusters of 12 to 150 members in this way (SCL 160, 114, 9 and 124 from the catalogue, as well as two random distributions of given symmetry with  $N_{cl} = 50$  and 150); several different realizations were done for each random exclusion. The results are presented for an example of the Shapley supercluster in Figure 2.

The left panels of Figure 2 show the variation of the parameters of the ellipsoid of concentration during the process of *randomly* excluding supercluster members. We see that the ellipsoid parameters are surprisingly stable: a reduction of the number of members down to  $\approx 30\%$

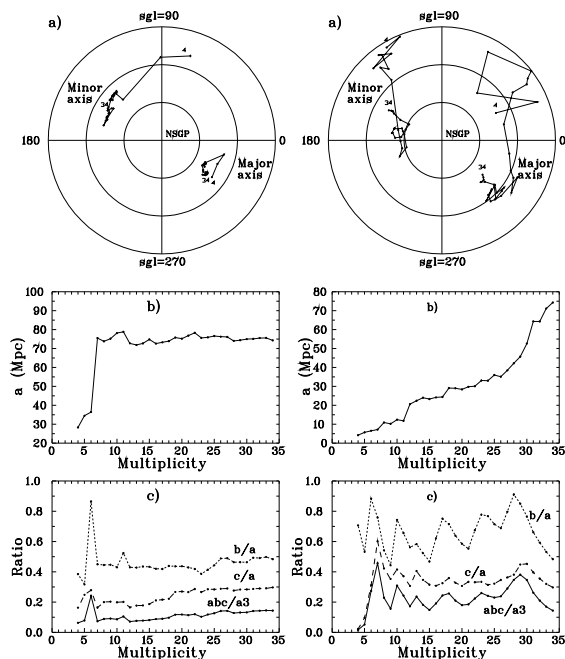


**Fig. 2.** The variation of supercluster parameters during exclusion of member clusters, shown here for the Shapley supercluster. Left panels correspond to random exclusion, right panels to the exclusion of the most distant cluster of the previous configuration. Panel (a) shows the direction of the major and the minor axis projected on the supagalactic northern hemisphere; panel (b) – the size of supercluster (semi-major axis); and panel (c) the axial ratios and ellipticities. The dots in panel (a) mark the direction of the minor and major axis for the Shapley supercluster as a function of the number of member clusters from 34 down to 4.

changes the main parameters by no more than  $\pm 10\%$  and the ellipsoid axes do not drift by more than  $10^\circ$ .

In the right panels of Fig. 2 the member clusters are excluded in the order of their distance from the supercluster centre, starting with the outermost one. In this case we see a rapid contraction of the ellipsoid accompanied by strong variations of its shape. However, the directions of principal axes is quite stable until the number of members is reduced down to about 8. The covariance matrix, and consequently, parameters of the ellipsoid of concentration, depend strongly on the most distant member clusters. A similar exercise of removing the innermost members shows that in this case the main parameters of the ellipsoid remain nearly unchanged.

These calculations show that the main parameters of the ellipsoid of concentration depend primarily on the location of the distant members of superclusters. The method discussed above can be used for superclusters with  $N_{cl} \geq 8$  members. For superclusters with  $N_{cl} = 5 \dots 7$  members we must take into account the fact that random

deviations of supercluster parameters due to poor determination of membership may be quite large.

We analysed also the possible influence of observational errors on the parameters of the ellipsoid of concentration. Redshift errors are typically less than 100 km/s, and have little influence on the ellipsoid. Errors due to the velocity dispersion of galaxies in clusters are larger, the median value is about 700 km/s (Mazure *et al.* 1996, and Andernach & Tago 1998). These errors may be important only for clusters whose mean velocity is based on one or a few galaxy redshifts. In those cases where the redshift is determined from the brightest members of clusters that lie in the dynamical centre of a cluster, these errors are much smaller. A possible source of errors are the peculiar velocities of clusters (Watkins 1997) and bulk motion of clusters with respect to the Hubble flow. If the bulk motion exists, then we can assume that clusters in the same supercluster have similar velocities, and that this error does not influence our results. To analyse the influence of peculiar velocities we shifted supercluster members randomly in velocity space up to  $\pm 700$  km/s, and recalculated the supercluster parameters from the revised membership of individual clusters. We found that these factors are noticeable only when they cause a removal of distant members from superclusters; in this case the changes are similar to those described above.

### 3.3. Comparison with previous studies

We compared our method with those used by West (1989) and ZZSV to derive the shapes of superclusters. These methods are also based on the covariance matrix, and describe the geometrical properties of superclusters in the same way. The main difference is the normalisation used by West: to avoid the possible bias by the outer members he divided local coordinates of clusters by the distance from the centre of the supercluster. In this way he projected all members of the supercluster to the sphere of unit radius surrounding the geometrical centre of the supercluster. We were afraid that using this method all information about the spatial dimensions of the supercluster would be lost. Nevertheless, our calculation of supercluster shape parameters according to West’s (1989) method showed that the orientation of superclusters (i.e. the direction of the major axes) were in most cases **exactly the same** as those according to our method; we found only three superclusters (of 42) where two of the main axes changed their order.

Differences in shape between the two methods are somewhat greater but not crucial: the ellipticities  $V/V_{sph} = bc/a^2$  differ by only a factor of 1.5 on average (superclusters are more elliptical according to our method). We conclude that the advantage of our method compared to West’s method is the estimation of spatial dimensions of superclusters.

#### 4. Geometrical properties of superclusters

In this Section we analyse geometrical properties of superclusters – their size and shape. For this purpose we use the length of the semi-major axis,  $a$ , the intermediate semi-axis,  $b$ , the semi-minor axis,  $c$ , and the ratios of axes,  $b/a$  and  $c/a$  and the ellipticity,  $e$ .

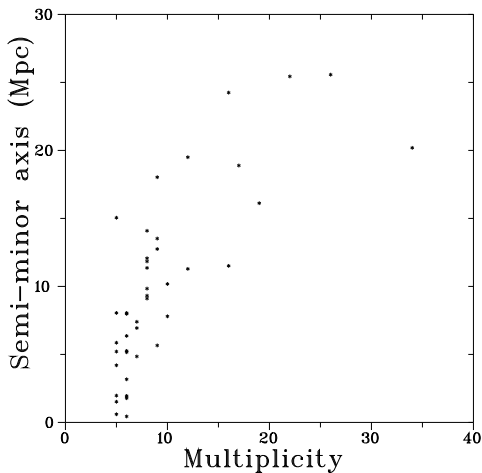


**Fig. 3.** The length of the semi-minor axis of the superclusters of different multiplicity  $N_{cl}$ .

Mean sizes of semiaxes for superclusters with multiplicity  $N_{cl} < 8$  and  $N_{cl} \geq 8$  are given in Table 1. In Figure 3 we show the semi-minor axis of the superclusters as a function of their richness.

The median length of the semi-minor axes  $c$  is  $10 h^{-1}$  Mpc, close to the value found by EETDA. The semi-minor axis of the “thinnest” superclusters (i.e. those with smallest value of  $c$  or with the highest ellipticity) is only  $0.4 h^{-1}$  Mpc, of the order of the radius of a normal Abell cluster. This supercluster, SCL 126, consists of a single elongated cluster filament; we shall discuss this supercluster in more detail in Section 5. The median value of the intermediate semiaxis  $b$  is  $20 h^{-1}$  Mpc.

**Table 1.** Median semiaxes ( $a$  and  $c$ ) of superclusters and the correlation lengths ( $r_0$ ) for clusters in superclusters (from paper II)

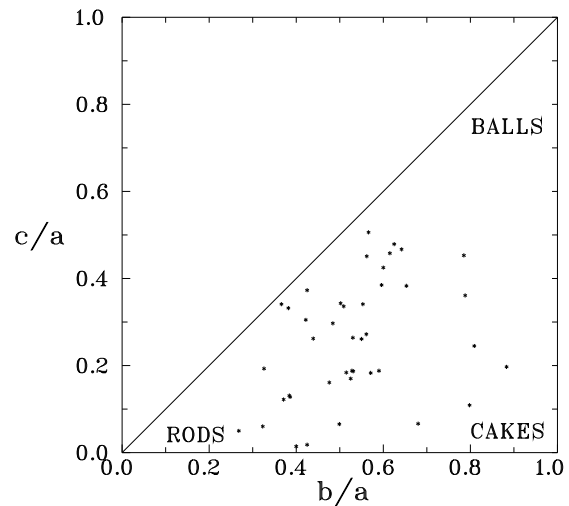
Multiplicity	$a$ $h^{-1}$ Mpc	$c$ $h^{-1}$ Mpc	$r_0$ $h^{-1}$ Mpc
$N_{cl} < 8$	31	5	17
$N_{cl} \geq 8$	42	12	46

Table 1 shows that the supercluster sizes depend strongly on their richness. A similar tendency was found for the correlation length,  $r_0$  (Papers II and III; the correlation length from Paper II is also given in the Table). In superclusters of small and medium richness the correlation length is approximately equal to the geometric mean

of the median values of the major and minor semiaxes while in very rich superclusters it is near to the median value of the semi-major axis. Thus we see that the correlation length characterises the size of superclusters in a slightly different manner than the size of semiaxes.

The location of superclusters in the  $c/a$  vs  $b/a$  plane is shown in Figure 4. We see that there are no superclusters with spherical shape. One of the roundest superclusters have axial ratios  $a:b:c = 1:0.5:0.5$  (the supercluster in Microscopium with ten members, SCL 174); the maximum density of points in Figure 4 corresponds to regions of axes ratios between  $1:0.5:0.2$  and  $1:0.6:0.4$ . The median ellipticity is 0.125; 40% of superclusters have  $e < 0.1$ , 75% less than 0.2, and there are no superclusters with  $e > 0.4$ .

Based on data for 11 superclusters West (1989) found that superclusters are flattened with typical axial ratios of  $1:0.3:0.3$  to  $1:1:0.3$  which agrees with our results rather well.



**Fig. 4.** The supercluster axis ratios  $c/a$  versus  $b/a$ . The corners of the triangle correspond to  $1:0:0$  (prolate shape),  $1:1:1$  (spherical shape) and  $1:1:0$  (oblate shape).

Thus our results show that the superclusters are quite flattened objects: the shape of superclusters can be described as “prolate” or “rods”, and “oblate” or “cakes”. Elongated “oblate” superclusters are more common than flattened “prolate” ones.

#### 5. Large scale orientation of superclusters

The strong elongation of superclusters allows us to find the spatial orientation of superclusters, and to study the correlation of the orientation with respect to some preferred direction, like the location of the observer, adjacent rich superclusters or voids, etc.

As pointed out above, we have no spherical superclusters in our sample. Consequently, the orientation of superclusters can be determined by the directions of the major

and minor axes. We shall calculate the distribution of the angles of supercluster axes with respect to directions mentioned above, and compare this with a uniform (or random) distribution.

### 5.1. Line-of-sight orientation

First we shall test for the presence of a possible observational bias that could reflect artefacts in the cluster catalogue, for instance the presence of projection effects in the cluster catalogue, or the influence of cluster peculiar velocities in superclusters. Distances of clusters are determined from their redshifts. Thus, if clusters in superclusters have a large dispersion of velocities with respect to the supercluster centres, then, using our method, superclusters will be elongated along the line of sight. Such a “finger of God” effect is observed in clusters of galaxies. Clusters are virialised objects and have large internal velocity dispersion of galaxies. Due to the large sizes of superclusters we do not expect the latter effect to be strong.

In Figure 5 we present the line-of-sight orientation of all superclusters with  $N_{cl} \geq 5$ . We see that both major and minor axes have a nearly isotropic distribution. The only deviation from the uniform distribution is a small excess at small values of cosines (histogram above the diagonal) corresponding to the major axis lying nearly perpendicular to the line of sight ( $\cos(ar) < 0.3$ , i.e.  $\angle ar > 70^\circ$ ). Surprisingly, among these “nearly perpendicular” superclusters there are three of the four most flattened systems (SCL 18, 126 and 202) – a fact, suggesting a possible influence of large-scale motions on the morphology of superclusters in redshift space. We discuss this phenomenon in Section 6. In any case no preferred line-of-sight orientations are present in our sample. The same was found also by West (1989) and by Zucca *et al.* (1993).

### 5.2. Orientation with respect to voids and superclusters

It is well known from observations and numerical simulations that the matter flows away from voids towards centres of large mass concentrations (Kaiser 1987, Gramann *et al.* 1993). Superclusters are the largest known mass concentrations in the Universe, thus one may assume that they are oriented with respect to adjacent voids (centres of divergence), or nearby superclusters (centres of convergence). For this purpose we checked the orientation of superclusters relative to the three richest superclusters in our catalogue with  $N_{cl} > 20$ . These very rich superclusters are the Shapley supercluster, the Sculptor supercluster, and the Horologium supercluster. To investigate the orientation of superclusters relative to voids we used the catalogue of voids by EETDA.

The results of this analysis showed no significant deviation from isotropy. The only deviation from the isotropic distribution is a weak tendency of perpendicularity of ma-

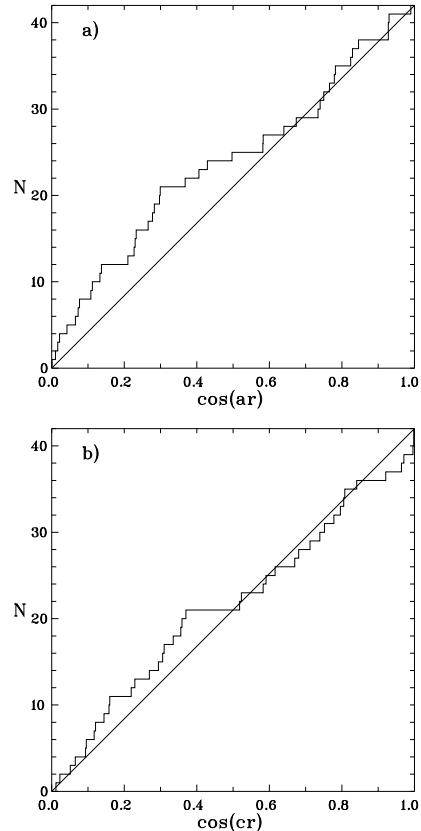


**Fig. 5.** The integrated distributions of cosines of angles of major axes (upper panel) and minor axes (lower panel) with respect to the line-of-sight vector. Small values of cosines (histogram above the diagonal) corresponds to the tendency for axes to be perpendicular to the main direction (line-of-sight vector); high values (histogram below the diagonal) suggest the directions to be parallel to the line of sight.

ior axes to the direction toward the centre of the Bootes void.

The absence of preferable orientations with respect to voids is somewhat surprising. Superclusters surround voids, thus at least superclusters at the edge of voids should be perpendicular to the direction of the void centres. However, a supercluster oriented perpendicular with respect to one void may be parallel to another one causing together the absence of preferred orientations. Our negative result may also be due to the small number of superclusters: there are 42 superclusters and 26 voids in our catalogue.

### 5.3. Global trends in orientation

Global orientations have been searched for in two ways: studying the distribution of direction cosines in Cartesian space, and searching the possible centre of convergence of

the supercluster axes. We select the supergalactic  $X$ –axis as the main direction because it is perpendicular to the Dominant Supercluster Plane (DSP, see Paper I). However, we found no preferential orientation, except for a very weak tendency of minor axes to be parallel to the  $X$ –axis (perpendicular to the DSP).

We tried to find a possible “centre of convergence”, independent of the visible structures in our sample. Such a centre could indicate the presence of a very large mass concentration outside our sample boundaries. We searched for such a centre in the following way: first we calculated the direction cosines of principal axes for all supercluster ellipsoids; then we derived the meeting-points (points at which the distance between the two lines is the shortest) of major axes for all possible pairs of superclusters. Thus we obtained 861 meeting-points for 42 superclusters and tried to find the common meeting-point as a concentration of them using cluster analysis. We found this point to lie close to the coordinate center, i.e. at the location of the observer; so the distribution of line-of-sight angles from this “new” viewpoint is almost the same as in Figure 5. We conclude that no such point of convergence exists; the directions of axes of the superclusters are distributed isotropically, and the clustering of meeting-points only reflects the central symmetry of our sample.

#### 5.4. Orientation of supercluster pairs in supercluster-void network

As we showed in Paper I, superclusters form a rather regular network with characteristic distance of about  $120 h^{-1}$  Mpc. This distance corresponds to the distance between superclusters at opposite void walls; about 75% of very rich superclusters have a neighbouring supercluster at this distance (typically, the second nearest neighbour).

As we mentioned in the Introduction, several different kinds of preferred orientations of galaxies and systems of galaxies have been found, among them the alignment of major axes of clusters in superclusters with the main ridge of superclusters. Therefore we checked whether such alignments extend over scales that characterize the supercluster-void network. To this aim we computed the orientations of superclusters with respect to their nearest three neighbours.

To test the method of finding supercluster orientations, as well as for comparison with orientations of real superclusters, we additionally generated a set of superclusters located on a regular 3-dimensional lattice oriented in the direction of the coordinate axes. In these sets the number of superclusters was equal to the number of observed superclusters, 42. The multiplicity matched the observed one, and the shapes of superclusters were elongated. The major axes of superclusters were aligned along the rods of the lattice (in the direction of three coordinate axes); the exact location of superclusters along the rods was random (we only avoided overlapping of superclusters located in

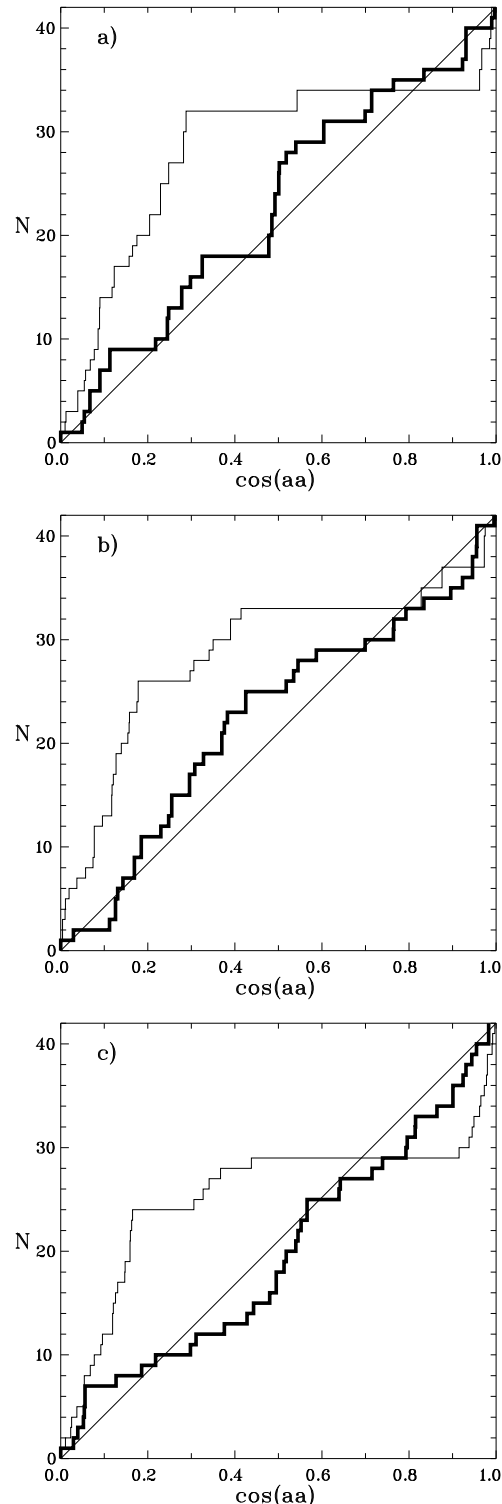


**Fig. 6.** Orientation of supercluster pairs: cosine of angles between major axes of neighbouring superclusters for the nearest neighbour (panel a), the second nearest (panel b) and the third nearest (panel c) neighbour. The thick histogram corresponds to observations, the thin histogram to model superclusters (see text), and the thin straight line shows a uniform distribution.

the same direction on the same rod). Therefore, for about 2/3 of superclusters the nearest neighbours are perpendicular to each other, and for the rest of them the nearest neighbours are parallel. Then we calculated orientations between real supercluster pairs, as well as between model superclusters (Figure 6).

As is seen in Figure 6, the relative orientations between model superclusters elongated along rods of a regular lattice show strong perpendicular and parallel orientations. Thus our method is able to detect preferable orientations. As shows the Kolmogorov-Smirnov test, the possibility that model superclusters could have random orientations can be rejected at 99% confidence level. Figure 6 shows also that the orientations between real supercluster pairs in the supercluster-void network are nearly random. The same is confirmed by the Kolmogorov-Smirnov test.

Summarising, we do not find any correlation or regularity in the spatial orientation of superclusters. The orientation of superclusters seems to be isotropic on all scales up to the sample volume.

## 6. Discussion

The fact that we have found no sign of peculiar motions of clusters within rich superclusters is not surprising since expected velocities must be of the order of the observationally known bulk motions of galaxies, 600 km/s (Branchini and Plionis 1996). An object having a peculiar velocity of 600 km/s, will travel about  $6 h^{-1}$  Mpc in a Hubble time relative to the general Hubble flow. Dimensions of superclusters exceed these distances many times. Numerical experiments also indicate that superclusters have the form and shape which is close to the form and shape during their formation (Frisch *et al.* 1995).

The isotropy of supercluster orientation with respect to the line of sight confirms that superclusters are still in the stage of formation. The lack of a line-of-sight elongation excludes the idea of gravitationally bound relaxed superclusters, where internal motions would lead to radially elongated “fingers of God”.

The lack of spherical superclusters is in harmony with the view that superclusters are not dynamically bound systems but parts of the supercluster-void network which as a whole is expanding with the Hubble flow. Numerical experiments show that in high-density regions clusters and groups of galaxies are concentrated to long chains. This phenomenon was detected empirically many years ago (Jöeveer and Einasto 1978, Jöeveer *et al.* 1978).

A weak tendency of major axes to be perpendicular to the line of sight is in agreement with theoretical predictions. Supercluster members are moving towards the centre of the supercluster, and line-of-sight dimensions of superclusters are decreased in redshift space (Kaiser 1987, Gramann *et al.* 1993).

In this connection we note that three very flat superclusters, mentioned in Section 3, are very elongated sys-

tems of 5 or 6 members. These are SCL 18, a relatively nearby supercluster in Phoenix ( $d \approx 82 h^{-1}$  Mpc), and superclusters 126 and 202, both at a distance of about  $240 h^{-1}$  Mpc. The list of members of these superclusters is given in Paper I. The dimensions of these superclusters in the plane of the sky exceed their line-of-sight dimension between 10 times (for SCL 18) and 30 times (for SCL 126). We note that all distances of their member clusters are determined spectroscopically with great accuracy. We suppose that the perpendicularity of these superclusters to the line of sight is enhanced and we see the effect of the matter inflow towards the centers of the superclusters. The possibility of such an effect has been discussed, for example, in Praton *et al.* (1997), where they show that the redshift effects may selectively enhance the appearance of the superclusters lying perpendicular to the line of sight. This shape reflects also the formation history of superclusters in the sense that clusters may be located along filaments and sheets (Colberg *et al.* 1997). A detailed dynamical study of these regions appears worth-while: as the nearest of them is at a distance of  $82 h^{-1}$  Mpc, the concentration of non-cluster galaxies to this plane should be visible.

## 7. Conclusions

We have studied geometrical properties of superclusters approximating their shape with an ellipsoid of concentration. Our main results can be summarised as follows.

i) Superclusters are elongated systems with characteristic axial ratios between 1:0.5:0.2 and 1:0.6:0.4. There are no spherical superclusters.

ii) We found no significant orientation of superclusters, neither towards the observer, nor the large voids, nor towards any other large-scale feature. Superclusters are oriented isotropically in space. There are no strong contaminations in the cluster catalogue that could cause preferable orientations of superclusters along the line of sight.

iii) The size of superclusters depends on their richness. This effect is similar to the dependence of the correlation length of clusters on the richness of superclusters they are located.

*Acknowledgements.* We thank the referee, Dr. G. Zamorani, for many useful comments which helped improve the paper. This work was supported by the Estonian Science Foundation (grant 182), by the International Science Foundation (grant LLF100), and by the Max-Planck-Gesellschaft. JJ would like to thank the Division of Astronomy and Physics of Estonian Academy of Sciences for financial support; JE was supported in Potsdam by the Deutsche Forschungsgemeinschaft; HA benefitted from financial support by CONACYT (Mexico; Cátedra Patrimonial, ref 950093).

## References

Abell, G., 1958, ApJS 3, 211



- Abell, G., Corwin, H., Olowin, R., 1989, ApJS 70, 1 (ACO)
- Andernach, H., Tago, E., Stengler-Larrea, E., 1995, *Astroph. Lett & Comm.* 31, 27
- Andernach, H., Tago, E., 1998, Proc. "Large Scale Structure: Tracks and Traces", eds. V. Müller, S. Gottlöber, J.P. Mückel, & J. Wambsganss, World Scientific, Singapore, in press; [astro-ph/9710265](#)
- Binggeli, B., 1982, AA 107, 338
- Branchini, E., Plionis, M., 1996, ApJ 461, L17.
- Colberg, J.M., White, S.D.M., Jenkins, A., Pearce, F.R., 1997, MNRAS, in press; [astro-ph/9711040](#)
- Djorgovski, S., 1983, ApJ 274, L7.
- Einasto, J., Einasto, M., Frisch, P., Gottlöber, S., Müller, V., Saar, V., Starobinsky, A.A., Tago, E., Tucker, D., Andernach, H., 1997c, MNRAS 289, 801, (Paper II)
- Einasto, J., Einasto, M., Frisch, P., Gottlöber, S., Müller, V., Saar, V., Starobinsky, A.A., Tucker, D., 1997d, MNRAS 289, 813, (Paper III)
- Einasto, J., Einasto, M., Gottlöber, S., Müller, V., Saar, V., Starobinsky, A. A., Tago, E., Tucker, D., Andernach, H., Frisch, P., 1997a, Nat 385, 139
- Einasto J., Jõeveer M. & Saar E., 1980, MNRAS 193, 503
- Einasto, M., Einasto, J., Tago, E., Dalton, G.B., Andernach, H., 1994, MNRAS 269, 301 (EETDA)
- Einasto, M., Tago, E., Jaaniste, J., Einasto, J., Andernach, H., 1997b, AAS, 123, 119 (Paper I)
- Flin, P., & Godlowski, W., 1986, MNRAS 222, 525
- Frisch, P., Einasto, J., Einasto, M., Freudling, W., Fricke, K.J., Gramann, M., Saar, V., & Toomet, O., 1995, AA 296, 611
- Gramann, M., Cen, R., & Bahcall, N., 1993, ApJ 419, 440
- Gregory, S.A., Thompson, L.A., & Tift, W., 1981, ApJ 243, 411
- Jaaniste, J., 1982, Tartu Astrophys. Obs. Publ., 49, 170
- Jõeveer, M., Einasto, J., 1978, in *The Large Scale Structure of the Universe*, IAU Symp. 79, eds. M.S. Longair, J. Einasto, Reidel, 409
- Jõeveer, M. Einasto, J., Tago, E., 1978, MNRAS 185, 35
- Kaiser, N., 1987, MNRAS 227, 1
- Lauer, T.R., & Postman, M., 1994, ApJ 425, 418.,
- Korn, G. A. & Korn, T. M., 1961. *Mathematical Handbook for Scientists and Engineers*, McGraw–Hill Book Co.,Inc.
- Mazure, A., Katgert, P., den Hartog, R., Biviano, A., Dubath, P., Escalera, E., Focardi, P., Gerbal, D., Giuricin, G., Jones, B., Le Fevre, O., Moles, M., Perea, J., Rhee, G., 1996, A&A, 310, 31
- Oort, J., 1983, ARA&A, 21, 373
- Plionis, M., Valdarnini, R., Jing, Yi-P., 1992, ApJ 398, 12
- Praton, E.A., Melott, A.L., McKee, M.Q., 1997, ApJ 479, L15
- Watkins, R., 1997. MNRAS, in press; [astro-ph/9710170](#)
- West, M., 1989, ApJ, 347, 610
- Zucca, E., Zamorani, G., Scaramella, R., Vettolani, G., 1993, ApJ 407, 470 (ZZSV)

## Appendix

**Table A1.** The shape and orientation of superclusters

(1)	(2)	(3)	(4)	(5)	(6)	(7)	(8)	(9)	(10)
No SCL	$N_{CL}$	$c$ Mpc	$b$ Mpc	$a$ Mpc	$V/V_{sph}$	$\angle(cx)$ deg	$\angle(ax)$ deg	$\angle(cr)$ deg	$\angle(ar)$ deg
3	8	9.1	25.8	48.6	.099	60	77	72	41
5	5	2.0	15.0	30.1	.033	26	65	84	76
9	22	25.4	29.2	76.6	.127	87	42	41	68
10	17	18.9	20.3	55.5	.125	56	45	37	54
18	6	1.8	18.2	26.7	.045	75	25	77	86
24	7	6.9	21.8	36.9	.111	63	41	47	83
30	8	14.1	21.4	42.0	.171	44	59	80	73
34	6	5.3	15.5	32.6	.077	89	29	76	88
48	26	25.6	35.1	54.7	.300	88	68	74	42
49	5	5.2	16.2	28.5	.105	83	25	3	87
65	5	15.1	19.6	31.5	.299	37	52	88	66
67	6	5.2	15.1	39.4	.050	38	57	51	38
91	9	13.5	21.9	39.6	.189	60	64	54	77
93	9	5.7	17.2	46.3	.045	60	43	38	85
107	8	12.1	17.0	28.4	.255	22	70	87	21
109	8	11.8	17.3	34.6	.172	31	68	83	8
111	16	24.2	42.1	53.6	.355	77	79	13	76
114	16	11.5	38.1	47.1	.198	86	17	42	47
124	34	20.2	32.9	67.9	.144	49	59	47	42
126	6	.4	12.5	31.3	.006	56	83	4	89
127	5	4.2	18.8	21.2	.174	29	76	15	76
128	6	2.0	10.5	32.4	.019	46	44	69	40
138	12	19.5	26.2	42.6	.282	47	81	68	21
150	10	10.2	17.4	26.6	.250	64	45	58	82
157	6	8.0	11.1	26.2	.129	48	45	70	85
158	8	9.8	16.5	37.6	.115	68	63	72	38
160	12	11.3	19.0	58.3	.063	72	26	84	60
164	5	5.9	18.1	34.5	.089	61	57	36	54
168	5	1.5	8.1	30.3	.013	43	57	80	21
170	7	4.8	13.6	26.4	.095	54	40	69	34
174	10	7.8	9.7	17.3	.253	69	86	71	50
188	9	12.8	14.5	34.1	.159	89	25	5	89
190	5	8.0	17.0	30.8	.144	73	41	81	73
192	8	11.4	24.8	31.5	.284	84	67	36	64
193	8	9.3	19.2	34.2	.153	31	58	83	72
197	9	18.0	20.1	35.6	.286	20	70	53	74
202	5	.6	14.1	33.3	.008	14	84	44	83
205	19	16.1	32.4	61.1	.140	12	85	86	32
208	6	6.4	19.1	49.5	.050	54	37	22	72
209	7	7.4	11.5	19.2	.230	57	66	32	82
210	6	8.0	22.6	42.9	.099	26	75	58	88
213	6	3.2	23.2	29.1	.087	65	79	89	34

Columns are as follows:

- 1) reference number from Table A1 in Paper I  $No$ ;
- 2) number of clusters  $N_{cl}$ ;
- 3 - 5) length of the three principal semiaxes of ellipsoid of concentration,  $c$ ,  $b$  and  $a$ ;
- 6) the ratio of the volume of the ellipsoid to the volume of a sphere of the same diameter  $V/V_{sph}$ ;
- 7, 8) angles of axes with the supergalactic  $X$ -axis  $\angle cx$ ,  $\angle ax$ ;
- 9, 10) angles of the minor and the major axis with the line-of-sight direction  $\angle cr$ ,  $\angle ar$ .